

Articles

Photoinduced Electron Transfer from Excited Ruthenium Complexes at Nanocrystalline TiO₂ Electrodes

Jong Hyun Bae, Donghwan Kim[†], Yeong Il Kim[†], and Kang-Jin Kim*

Department of Chemistry, Korea University, Seoul 136-701, Korea

[†]Division of Material Science and Engineering, Korea University, Seoul 136-701, Korea

*Department of Chemistry, Pukyong National University, Pusan 608-737, Korea

Received October 30, 1996

Photoinduced electron transfer from the charge-transfer excited states of Ru(tpy)(bpy(COOH)₂)CN⁺, Ru(tpy)(bpy(COOH)₂)Cl⁺, Ru(tpy)(bpy(COOH)₂)H₂O²⁺, and Ru(tpy)(bqu(COOH)₂)Cl⁺ to the conduction band of TiO₂ has been studied through photoelectrochemical methods. Ru(tpy)(bpy(COOH)₂)CN⁺ produced the highest current density and open-circuit photovoltage, whereas Ru(tpy)(bqu(COOH)₂)Cl⁺ produced the lowest values. A potential barrier was employed to explain the experimental result that the rate of the electron transfer increases with increasing the energy difference between the donor and acceptor. A sensitizer with a high current density yielded a high photovoltage and a high conversion efficiency. The reduction rate of the oxidized sensitizer decreased with the increases in the reduction potential of the sensitizer, resulting in a poor stability of a photoelectrochemical cell.

Introduction

Titanium dioxide (TiO₂) has an exceptional thermal and photochemical stability against corrosion, but its large bandgap ($E_g \approx 3.1$ eV) reduces enormously the fraction of solar radiation that can be harvested. The spectral response can be improved by using electronically excited states of dye molecules, on the ground that the excited states must have sufficient negative redox potentials that dye molecules can transfer electrons into the conduction band of TiO₂. This sensitization of large bandgap semiconductors using colored dye molecules with the hope of obtaining improved solar energy conversion efficiencies has been investigated for many years.¹⁻³

In recent years, there has been significant progress using metal complexes coated on a polycrystalline TiO₂ film which was prepared to maximize its surface area.^{4,5} Grätzel and co-workers⁵ reported that TiO₂-electrodes coated with *cis*-di(thiocyanato)-bis(2,2'-bipyridyl)-4,4'-dicarboxylate ruthenium(II) was found to be the most efficient amongst a series of ruthenium-containing dyes. The adsorbed dyes act as charge-transfer sensitizers. Very high incident photon-to-current conversion efficiencies as large as 10% have been achieved.⁵ However, the sensitizer desorbs in aqueous solution above pH 5. To ensure a strong adsorption on TiO₂ surface, transition metal dyes containing phosphonate groups were synthesized, but they did not allow more efficient charge separation at TiO₂.⁶⁻⁸ Further investigation on the synthesis of more efficient dyes needs to be pursued.

Over the years a number of physical methods have been applied to study the mechanism of dye sensitization of TiO₂ electrodes.⁹⁻¹¹ The methods can be divided into photoelectrochemical and spectroscopic ones. Photoelectrochemical methods establish that injection of charge carriers occurs

from the excited state of the dye to the conduction band of TiO₂, but do not say anything about the identity of the dye's excited state involved.

To understand the energetics at the dye/TiO₂ interface, in this article, we examine the photoelectrochemical behavior of nanocrystalline TiO₂ electrodes sensitized by synthesized ruthenium complexes in acetonitrile solution containing I⁻/I₃⁻. Nanocrystalline TiO₂ electrodes were prepared by sintering spin-coated TiO₂ films,⁵ and several ruthenium complexes with similar structures were synthesized. In addition, an attempt was made to elucidate the electron transfer mechanism from the excited charge-transfer states of the dyes to the conduction band of TiO₂.

Experimental

Materials

TiO₂ was obtained from Degussa AG (P-25: 30% rutile, 70% anatase). Triton X-100 was obtained from Aldrich and acetylacetone was obtained from Junsei. RuCl₃·xH₂O and 2,2':6,2''-terpyridine(tpy), 2,2'-bipyridine-4,4'-dicarboxylic acid (bpy(COOH)₂) and 2,2'-biquinoline-4,4'-dicarboxylic acid (bqu(COOH)₂) were purchased from Aldrich, Alfa, and Fluka, respectively. LiI and I₂ used as electrolytes were obtained from Junsei. All other materials obtained from Aldrich were used without further purification.

Preparation of Nanocrystalline TiO₂ Electrodes⁵

Commercial TiO₂ (3.00 g) was ground in a porcelain mortar with 1.00 mL of water containing 0.10 mL of acetylacetone to prevent reaggregation of the particles. After the TiO₂ powder was dispersed in the viscous paste, it was diluted by slow addition of 7.50 mL of water under continued grinding. Finally 0.020 mL of Triton X-100 was added to

facilitate the spreading of the colloid on the substrate. Using this solution, a 6 μm TiO_2 film was coated on ITO glass (Samsung Corning) by a spin-coating method at 3000 rpm and annealed at 500 $^\circ\text{C}$ in air for 1 hr.

Ga-In eutectic was rubbed on ITO in order to form ohmic contact with Cu wire. The contacts and the exposed edges of the electrode were insulated with an epoxy (K-epoxy, McKim Group). The area of the TiO_2 electrodes exposed to light was typically 1.0 cm^2 .

Synthesis of Ruthenium Complexes

[Ru(tpy)Cl₃](III)¹⁵. A 2.080 g amount of $\text{RuCl}_3 \cdot x\text{H}_2\text{O}$ and 0.240 g of 2,2':6'2"-terpyridine were heated at reflux for 4 hr in 250 mL absolute ethanol. Dark brown solid was collected from the red solution and washed with 30 mL of acetone, 50 mL of ether, and air-dried.

[Ru(tpy)(bpy(COOH)₂)Cl]Cl¹⁵. A 0.50 g quantity of Ru(tpy)Cl_3 and 0.30 g of 2,2'-bipyridine-4,4'-dicarboxylic acid were heated at reflux for 5 hr in 250 mL of 75% EtOH/25% H_2O containing 0.08 g of LiCl and 0.5 mL of triethylamine as a reductant. The pot contents were filtered hot and their volume was reduced to ~10 mL with a rotary evaporator, followed by chilling in a refrigerator for 24 hr. The solid was collected on a frit and washed with 50 mL ether and air-dried.

[Ru(tpy)(bqu(COOH)₂)Cl]Cl. The preparation was carried out by using the same procedure as for [Ru(tpy)(bpy(COOH)₂)Cl]Cl, substituting 2,2'-biquinoline-4,4'-dicarboxylic acid for the 2,2'-bipyridine-4,4'-dicarboxylic acid ligand.

[Ru(tpy)(bpy(COOH)₂)H₂O]Cl₂¹⁵. A 0.2 g amount of [Ru(tpy)(bpy(COOH)₂)Cl]Cl and 0.1 g of AgClO_4 were heated together at reflux for 1 hr in 100 mL of 75% acetone/25% H_2O . The solution volume was reduced to 10 mL with a rotary evaporator. The product was recrystallized in ethanol.

[Ru(tpy)(bpy(COOH)₂)CN]CN₅. A 0.3 g of [Ru(tpy)(bpy(COOH)₂)Cl]Cl and a 10-fold excess of KCN were heated at reflux and the solution volume was reduced with a rotary evaporator. The product was collected on a frit and recrystallized in ethanol.

Adsorption of ruthenium complexes to a TiO_2 electrode⁵. Each of ruthenium complex (0.010 g) was dissolved in 20 mL ethanol. Coating of the TiO_2 surface with a dye was carried out by soaking the TiO_2 film for 12 hr in the dye solution. It was resoaked in absolute ethanol to remove non-adsorbed dye molecules for 3 hr. The absorbance of adsorbed dye was determined by a UV-vis spectrophotometer.

Instruments and set-up

Photocurrents and cyclic voltammograms were obtained with an EG & G potentiostat/galvanostat M273. An Oriol 250W quartz tungsten halogen lamp (QTH) was served as a light source in conjunction with a Hitachi 390 nm cut-off filter to remove ultraviolet radiation. Light intensity was calibrated against a Newport 18/5-C power meter. The TiO_2 electrodes were illuminated in a three-electrode, one-compartment cell with a Pt mesh counter electrode and a Ag/AgCl reference electrode. The cell was made of pyrex fitted with 3 cm water jacket. In order to obtain monochromatic

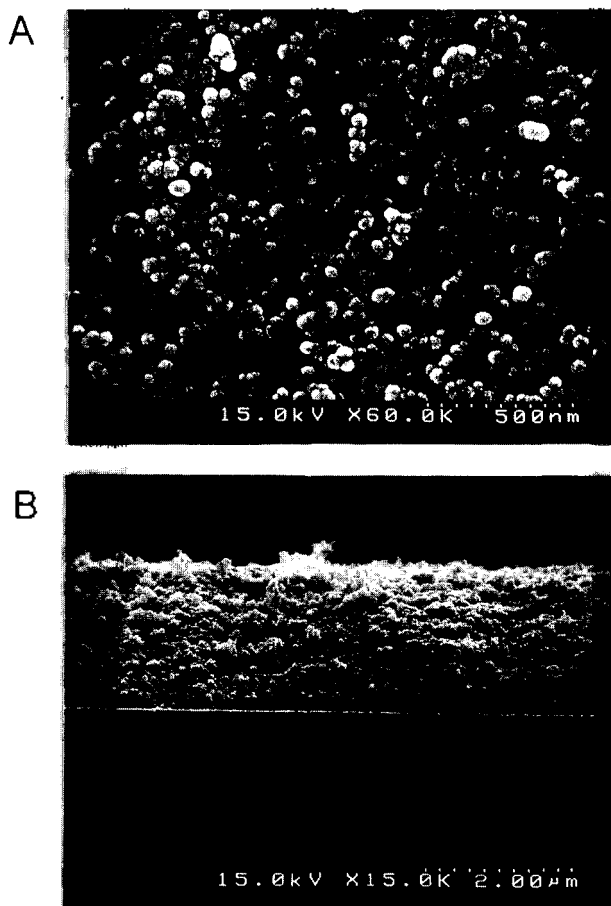


Figure 1. Scanning electron micrographs of a TiO_2 electrode deposited on a conducting glass. Magnification: (A) $\times 60,000$ (B) $\times 15,000$.

light a Bowman Series 2 luminescence spectrometer was used and UV-vis spectra were obtained with a Hewlett Packard 8452A diode array spectrophotometer. An ISI-SX-30E scanning electron microscope was employed to study the TiO_2 electrode surface and its thickness.

Results and Discussion

TiO_2 Film Characteristics

Figure 1 shows typical scanning electron micrographs of a TiO_2 film prepared by spin-coating colloidal TiO_2 particles on a conducting glass followed by annealing for 1 hr at 500 $^\circ\text{C}$. The sizes of TiO_2 particles in the film are quite uniform and estimated to be about 30–45 nm in diameter. The thickness of the TiO_2 films increases with the number of spin coating. The average thickness per spin coating was measured to be about 0.6 μm . With an increase in the film thickness the absorption spectra of the TiO_2 films show a red shift (Figure 2a). The absorbances at longer wavelengths are due to the decrease in transmittance caused by a somewhat hazy nature of the film. The absorbance of the dye-coated TiO_2 film corrected for the TiO_2 absorption and divided by the molar absorptivity yielded the surface dye concentration of about 2.3×10^{-7} mol/ cm^2 for a 6 μm -thick TiO_2 film. The photoelectrochemical behavior of spin-coat-

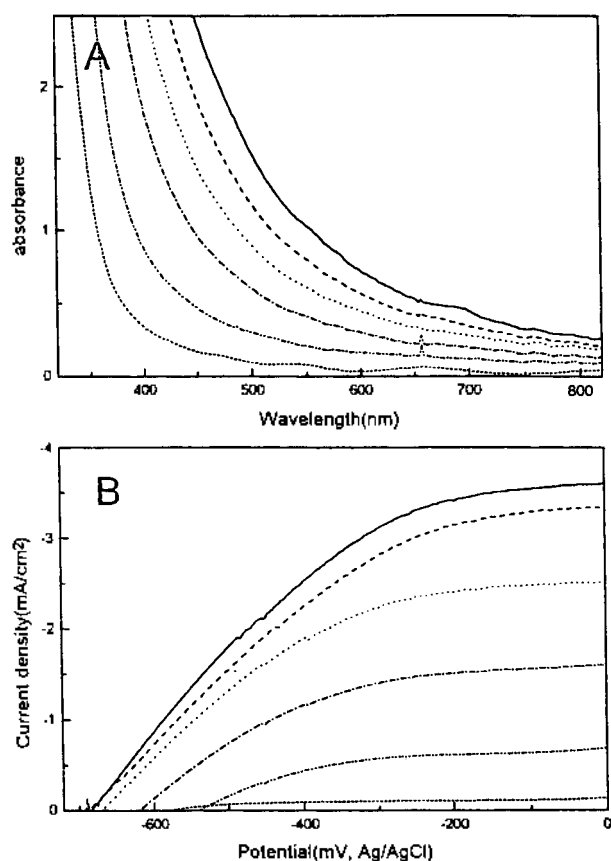


Figure 2. UV-vis spectra of bare TiO₂ electrodes and (B) current density-potential curves of Ru(tpy)(bpy(COOH)₂CN)⁺/TiO₂ anodes vs. film thickness in 0.3 M LiI/0.03 M I₂ acetonitrile solution at 100 mW/cm². — (9.0 μm), --- (7.2 μm), (5.4 μm), - - - (3.6 μm), - · - · (1.8 μm), ····· (0.6 μm).

ed TiO₂ films was studied by monitoring the photocurrent generated in a cell that employed a TiO₂ photoanode, a Pt mesh counter electrode, and I⁻/I₃⁻ as the redox electrolyte in acetonitrile. Figure 2b displays the current densities vs. applied potential of the TiO₂ film with different thickness using a ruthenium complex Ru(tpy)(bpy(COOH)₂CN)⁺ as a sensitizer. Higher current densities were obtained with the increase in the film thickness due to the increased adsorption of the ruthenium complex on the TiO₂ particles having high porosity and surface-to-volume ratio. A roughness factor, defined as the ratio between the real and projected surface of the film, of about 1000 has been obtained.² It appears to be desirable to have a thick film of TiO₂ in a photoelectrochemical cell in order to have a high photocurrent. However, as the thickness increases the injected electrons from the excited ruthenium complexes into the conduction band of TiO₂ become more difficult to migrate to the ITO substrate, and become easier to recombine with the oxidized ruthenium complexes or with oxidized species in the electrolyte solution. Similar explanation may be applied to the open-circuit photovoltage, V_{oc} , which is the voltage obtained at zero current density. The results in Figure 2b illustrates that V_{oc} reaches a steady value, about 0.68 V, beyond which the enhanced recombination appears to compensate with the increase in the injected electrons.

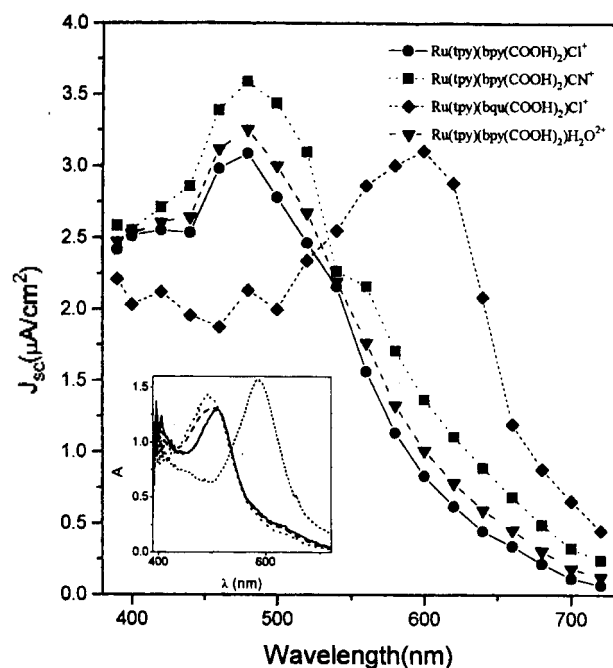


Figure 3. Photocurrent action spectra of Ru complex-sensitized TiO₂ electrode in 0.3 M LiI/0.03 M I₂ acetonitrile solution. The inset shows the absorption spectra of Ru complexes adsorbed on TiO₂ electrodes.

The current action spectra obtained with the TiO₂ films coated with the four ruthenium complexes are shown in Figure 3. Also shown are the absorption spectra of the dye-coated TiO₂ films. The photocurrent action spectra resemble their absorption spectra, indicating that under visible light illumination the ruthenium sensitizers are excited and the photogenerated electrons are transported efficiently to ITO through the nanocrystalline TiO₂ film.

Dye-Sensitization

Figure 4 shows the current density-voltage characteristics obtained with a photoelectrochemical cell that employed 6 μm thick, spin coated TiO₂ in 0.3 M LiI/0.030 M I₂ acetonitrile under visible-light illumination at 45 mW/cm² as described in Experimental. The TiO₂ electrodes were coated with the ruthenium sensitizers prior to the measurement of the photoelectrochemical behavior. The results of Figure 4 are tabulated in Table 1 with respect to the open-circuit voltage V_{oc} , short-circuit current density J_{sc} , fill factor ff , and conversion efficiency η . Table 1 also includes the half-wave potentials $E_{1/2}$ of the ruthenium complexes which were obtained by cyclic voltammetry in 1.0 M LiClO₄ acetonitrile.

The data in Table 1 show that among the sensitizers studied Ru(tpy)(bpy(COOH)₂CN)⁺ yielded the largest V_{oc} , J_{sc} , and η whereas Ru(tpy)(bqu(COOH)₂Cl produced the least conversion efficiency.

The variations in J_{sc} for the sensitizers can be attributed to the difference in the rate of heterogeneous charge transfer from the excited sensitizer, the donor, to the conduction band of TiO₂ the acceptor. For the electron transfer, there exists a free energy of activation for which the rate of the electron transfer is maximal. Under the present experimental conditions, we may assume that the Coulombic interactions

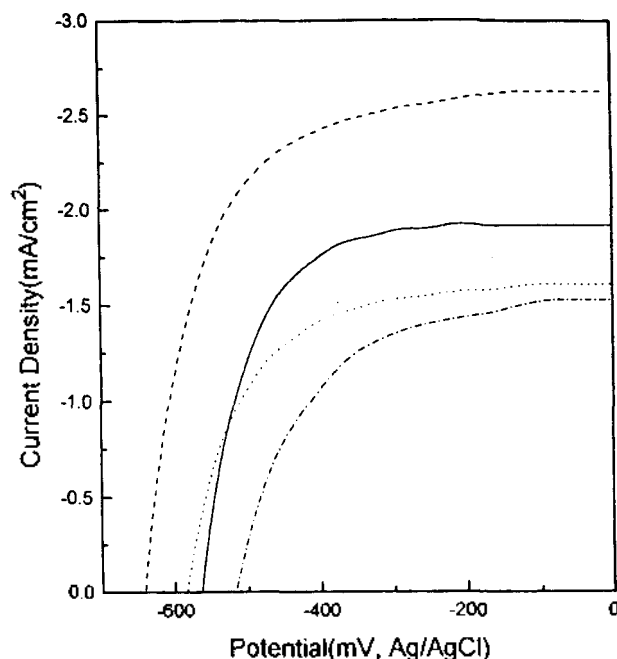


Figure 4. Photocurrent density-potential curves of Ru complexes adsorbed on the TiO_2 electrodes in 0.3 M LiI/0.03 M I_2 acetonitrile solution at 45 mW/cm^2 light intensity. — $\text{Ru}(\text{tpy})(\text{bpy}(\text{COOH})_2)\text{H}_2\text{O}^{2+}$, ---- $\text{Ru}(\text{tpy})(\text{bpy}(\text{COOH})_2)\text{CN}^+$, $\text{Ru}(\text{tpy})(\text{bpy}(\text{COOH})_2)\text{Cl}^+$, - · - · $\text{Ru}(\text{tpy})(\text{bqu}(\text{COOH})_2)\text{Cl}^+$.

between the cationic ruthenium complexes and the TiO_2 electrode are essentially the same and the ruthenium complexes are anchored to the TiO_2 surface by the carboxylate groups in the bipyridyl ligands. In addition, we may neglect the differences in the regeneration of the oxidized dyes by the electron transfer from iodide ions, because of relative slowness of the back reaction,² and because of nearly identical ionic atmospheres around ruthenium in the sensitizers of similar size with respect to the access of iodide ions. Figure 5 represents the energy level of the conduction band edge and the Fermi level of TiO_2 . Also shown are the ground and the excited state levels of the sensitizers which were established by cyclic voltammetry and absorption spectroscopy, respectively (Table 1). The energy difference between the two levels of the sensitizer approximately corresponds to the absorption maximum wavelength. The sensitizer $\text{Ru}(\text{tpy})(\text{bpy}(\text{COOH})_2)\text{CN}^+$ has the largest energy difference possibly because CN^- is a stronger ligand than Cl^- or H_2O in the spectrochemical series. It is immediately evi-

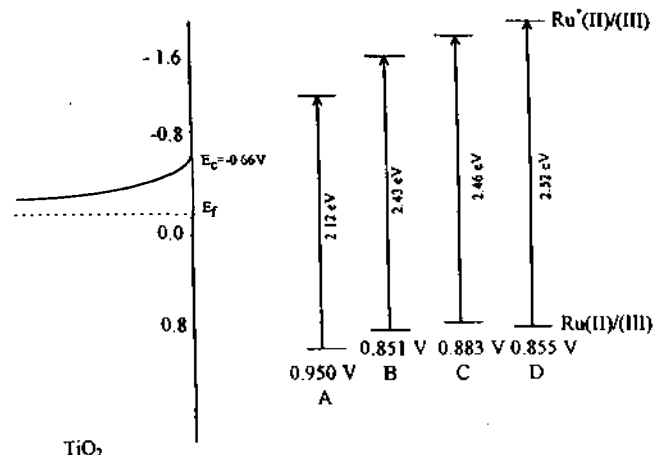


Figure 5. Interface energetics for TiO_2 thin films and Ru complexes in acetonitrile. A: $\text{Ru}(\text{tpy})(\text{bqu}(\text{COOH})_2)\text{Cl}^+$, B: $\text{Ru}(\text{tpy})(\text{bpy}(\text{COOH})_2)\text{Cl}^+$, C: $\text{Ru}(\text{tpy})(\text{bpy}(\text{COOH})_2)\text{H}_2\text{O}^{2+}$, D: $\text{Ru}(\text{tpy})(\text{bpy}(\text{COOH})_2)\text{CN}^+$.

dent on inspecting Table 1 and Figure 5 that the highest current density was obtained with the sensitizer whose excited state energy lies farthest from the conduction band edge of TiO_2 , whereas the lowest current density was obtained with the sensitizer lying closest to the conduction band edge. The increasing order of the current density of ruthenium dyes agrees well with the increase in the energy difference of the dyes. Therefore the energy difference between the conduction band edge and the excited state of the sensitizer can be regarded as a measure of the rate of the heterogeneous electron transfer.

The current density data can be interpreted by employing the free energy of activation, ΔG^\ddagger_{et} , a potential barrier associated with the heterogeneous electron transfer from the excited sensitizer to TiO_2 . The existence of a potential barrier is not unreasonable since the electron transfer should involve the injection of electrons from the bipyridyl ligand through the carboxylate group into the conduction band of TiO_2 .

For the case of photoinduced electron transfer on a semiconductor the rate of electron transfer can be described as,¹⁶

$$k \propto \exp(-\Delta G^\ddagger_{et}/RT) \quad (1)$$

where ΔG^\ddagger_{et} is the free energy of activation for the electron transfer and is related to the driving force, ΔG_{et} , which is the energy difference between the excited state and the conduction band of TiO_2 ,¹⁷

$$\Delta G^\ddagger_{et} = \frac{\lambda}{4} \left(1 + \frac{\Delta G_{et}}{\lambda} \right)^2 \quad (2)$$

where λ is defined as the total reorganization energy. This parameter can be separated into two terms, $\lambda = \lambda_v + \lambda_s$, where λ_v refers to the energy changes accompanying changes in bond lengths and bond angles during the electron-transfer step and λ_s refer to the energy change as the solvent shells surrounding the reactants rearrange. However, the variations of λ_s in identical solution are apparently insignificant since the radii of the sensitizers are very much the same. Thus

Table 1. V_{oc} , J_{sc} , ff , and $E_{1/2}$ (mV vs Ag/AgCl) of TiO_2 electrodes sensitized by ruthenium complexes. Incident light intensity was 45 mW/cm^2

| Complex | V_{oc} (V) | J_{sc} (mA/cm^2) | ff | $E_{1/2}$ ^a | η (%) |
|---|-----------------|---|------|------------------------|------------|
| $\text{Ru}(\text{tpy})(\text{bpy}(\text{COOH})_2)\text{Cl}^+$ | 0.59 | 1.8 | 0.54 | 851 | 1.3 |
| $\text{Ru}(\text{tpy})(\text{bpy}(\text{COOH})_2)\text{CN}^+$ | 0.64 | 2.7 | 0.52 | 855 | 2.0 |
| $\text{Ru}(\text{tpy})(\text{bpy}(\text{COOH})_2)\text{H}_2\text{O}^{2+}$ | 0.57 | 2.1 | 0.54 | 833 | 1.4 |
| $\text{Ru}(\text{tpy})(\text{bqu}(\text{COOH})_2)\text{Cl}^+$ | 0.52 | 1.5 | 0.51 | 950 | 0.9 |

^a in mV measured from 0.1 M LiClO₄, acetonitrile.

ΔG^\ddagger should be a function of the differences in equilibrium bond distances between the sensitizer and its oxidized species, and the force constants for all the vibrations of a reactant and product molecule.¹⁶ Apparently, in the present system, λ in a collective manner is somehow manifested to make ΔG^\ddagger_{et} smaller as ΔG_{et} becomes larger for the ruthenium complexes. Then it is expected that the higher the energy of the excited state, the smaller the effective potential barrier, and the larger is the current density. The back reaction is known to be much smaller compared with the electron-transfer reaction.² The applied potential provides a driving force for electron collection and prevents the charge recombination. Depending on the direct coordination of the sensitizer molecules onto the surface of TiO₂, the excited state of the sensitizer can be stabilized in comparison with the level predicted from the absorption spectrum. Then the potential barrier can be significantly lowered.

The maximal attainable photovoltage is the difference between the quasi Fermi level of TiO₂, F_n , and the electrochemical potential of the electrolyte I^-/I_3^- , E_{redox} .² Variation in the measured V_{oc} (Table 1) therefore resulted from the difference in the quasi Fermi level, which was caused by the non-equilibrium stationary concentration of the conduction band electrons during illumination, n^* . The rise of F_n with respect to E_{redox} is possibly expressed by¹⁸

$$F_n - E_{redox} \approx kT \ln \frac{\Delta n}{n_0} \quad (3)$$

where $\Delta n = n^* - n_0$ and n_0 is the concentration of the conduction band electrons under equilibrium in the dark. Since Ru(tpy)(bpy(COOH)₂)CN* produced the highest current density, its Δn is expected to be largest under the open circuit. As a consequence, V_{oc} of Ru(tpy)(bpy(COOH)₂)CN* should be the largest. Similarly, the smallest V_{oc} of Ru(tpy)(bpy(COOH)₂)Cl* can be related to its lowest current density among the sensitizers studied.

The plots in Figure 6 were based on the experimental data obtained for the dependence of current density-potential curves on the incident light intensities. From the plots a linear relationship between V_{oc} and $\log(J_{sc})$ holds up to about 7 mA/cm² for Ru(tpy)(bpy(COOH)₂)CN* and about 3 mA/cm² for other ruthenium complexes. The observation of the linear relationship suggests that the present photoelectrochemical cells under sub-bandgap illumination behave similarly to a diode under forward bias. Under open circuit, the photogenerated current is balanced by the recombination current. The open circuit photovoltage (V_{oc}) is related with J_{sc} by^{5,19,20}

$$V_{oc} = \frac{AKT}{q} \ln \frac{J_{sc}}{J_0} \quad (4)$$

where A is a parameter known as the diode quality factor, and J_0 is the saturation current density.²⁰ The value of A is dependent upon the transport mechanism that controls J_0 . With the aid of Eq. 4, the diode quality factors are obtained from the linear range of the plots in Figure 6, and found to be 2.3 ± 0.1 for all the ruthenium complexes. The number of investigations that report the diode quality factor for regenerative photoelectrochemical cells is limited.^{5,12,20} Recently, in similar studies to ours using *cis*-di(thiocyanato)bis(2,2'-bipyridyl-4,4'-dicarboxylate)ruthenium(II) as a sensitiz-

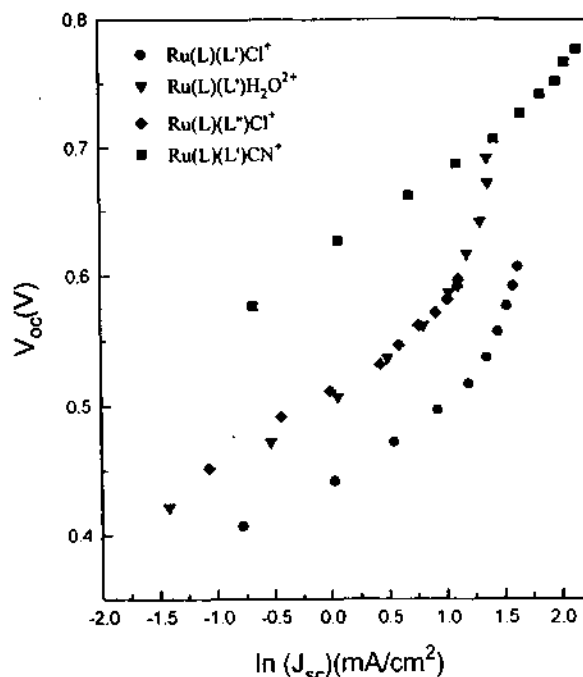
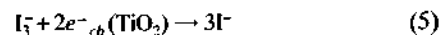


Figure 6. Plot of open-circuit potentials of dye/TiO₂ electrodes against short-circuit currents. L=terpyridine, L'=2,2'-bipyridine-4,4'-dicarboxylic acid, L''=2,2'-biquinoline-4,4'-dicarboxylic acid.

er, Nazeeruddin *et al.* described the performance characteristics of a TiO₂ cell where the diode quality factor was not given explicitly, but deduced to be about 1.4.⁵ Their explanation was mainly concerned with the recombination current caused by the reduction of triiodide ions in the electrolyte by the conduction band electrons,



Triiodide ion can penetrate into the nanometer-sized pores due to its relatively small size. However, if this recombination mechanism dominates, the diode quality factor should be 1.0¹³ instead of 1.4. The discrepancy arises because the current does not flow predominantly by the triiodide reduction. This discrepancy and the even larger A obtained in this study imply that other recombination mechanisms should participate in the present system. With a slightly different type of ruthenium dye, Smestad measured A=1.6.¹² This rather high value of A was attributed to both the triiodide reduction (Eq. 5) and the back reaction of the electron injection via recombination centers and surface states. Perhaps the surface recombination by trapping centers would be worthwhile to investigate extensively.¹⁹

Figure 7 shows the conversion efficiencies as a function of incident light intensity. Because we did not take into account the loss of light intensity due to the reflection off the glass surface of the photoelectrochemical cell and light absorption by the redox electrolyte, the relative conversion efficiencies of the TiO₂ electrodes were considered to be more relevant in this study. For all light intensities, Ru(tpy)(bpy(COOH)₂)CN* showed the highest conversion efficiencies, whereas Ru(tpy)(bpy(COOH)₂)Cl* had the lowest conversion efficiencies, except for the low light intensity region, which is consistent with the data present above. At

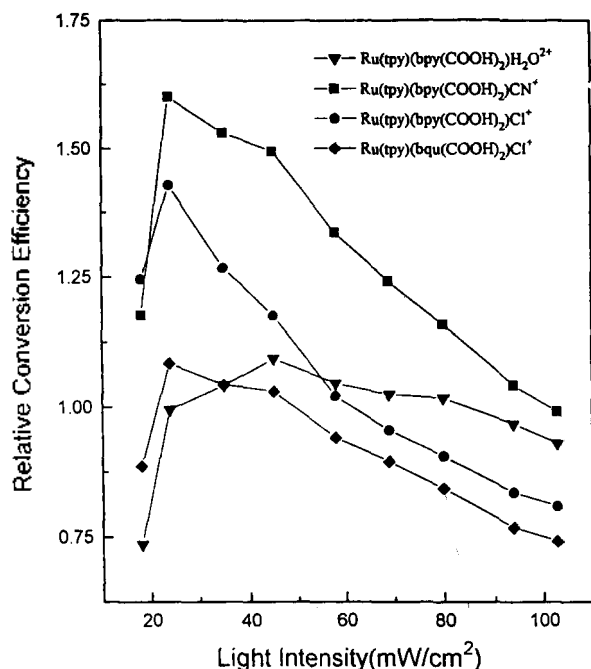


Figure 7. Dependence of light-to-current conversion efficiencies on incident light intensity.

higher intensities (above approximately 45 mW/cm²) under the present conditions the conversion efficiencies fall off rapidly, suggesting that the recombination of the injected electrons prevails over the diffusion by the conduction band electrons toward the TiO₂/ITO interface.

Stability of the Photocurrent

In order to examine the stability of the photoelectrochemical cell, the time dependence of the current density was measured. With the sensitizer Ru(tpy)(bqu(COOH)₂)Cl⁻ we observed that the current density decreased by about 86% during the first 60 min period, while the other three sensitizers possessing bipyridyl ligands showed about a 55% decrease under the same conditions. The poor stabilities can mainly be attributed to the accumulation of oxidized dyes on the TiO₂ surface and the slow regeneration of reduced dyes by the electron transfer from I₃⁻. Since Ru(tpy)(bqu(COOH)₂)Cl⁻ is expected to have a more hydrophobic atmosphere than the other dyes, the accumulation will be largest. Another possibility for the fast decay of the current density may arise from the complexation of I₃⁻ with the oxidized Ru(II) complexes, which hinders the electron transfer. Upon prolonged illumination, the degradation of Ru(II) complexes may also contribute to the poor stabilities. Further studies are needed to clarify the causes.

Conclusion

Dye-sensitized photocurrent densities were measured from nano-crystalline TiO₂ in acetonitrile. Ru(tpy)(bpy(COOH)₂)CN⁻ showed higher photocurrent density than other ruthenium complexes of similar structure. The results were interpreted by employing a potential barrier between the charge transfer excited state of a dye and the conduction band of TiO₂. The potential barrier should be a complex

function of the energy change accompanying predominantly the changes in chemical bond lengths during the electron transfer step. The energy change as the solvents around the reactants rearrange is insignificant. Ru(tpy)(bpy(COOH)₂)CN⁻ also produced a higher open-circuit photovoltage than the other sensitizers, implying that the quasi Fermi level lies the highest. A high diode quality factor suggests that a surface recombination process by trapping centers and surface states should be included in the recombination mechanism in addition to the reduction of triiodide by the injected conduction band electrons.

Acknowledgment. This work was supported by the Korea Science and Engineering Foundation (94-0501-05-01-3) and partially by the Ministry of Trade, Industry and Energy.

References

- Grätzel, M.; Kalyanasundaram, K. In *Photosensitization and Photo-catalysis Using Inorganic and Organometallic Compounds*; Klumer Academic Publ.: Dordrecht, The Netherlands, 1993; p 247.
- Hagfeldt, A.; Grätzel, M. *Chem. Rev.* **1995**, *95*, 49.
- Tan, M. S.; Laibinis, P. E.; Nguyen, S. T.; Kesselman, J. M.; Stanton, C. E.; Lewis, N. S. In *Progress in Inorganic Chemistry*; Karlin, K. D., Ed.; John Wiley: New York, USA, 1994; Vol. 41, p 21.
- O'Regan, B.; Grätzel, M. *Nature(London)*, **1991**, *353*, 737.
- Nazeeruddin, M. K.; Kay, A.; Humphry-Baker, R.; Müller, E.; Liska, P.; Vlachopoulos, N.; Grätzel, M. *J. Am. Chem. Soc.* **1993**, *115*, 6382.
- Bonhôte, P.; Moser, J. E.; Vlachopoulos, N.; Walder, L.; Zakeeruddin, S. M.; Humphry-Baker, R.; Grätzel, M. *Chem. Commun* **1996**, 1163.
- Péchy, P.; Rotzinger, F. P.; Nazeeruddin, M. K.; Kohle, O.; Zakeeruddin, S. M.; Humphry-Baker, R.; Grätzel, M. *J. Chem. Soc. Chem. Commun* **1995**, 65.
- Vogel, R.; Hoyer, P.; Weller, H. *J. Phys. Chem.* **1994**, *98*, 3183.
- Spitler, M. T.; Calvin, M. *J. Chem. Phys.* **1977**, *66*, 1294.
- Kay, A.; Humphry-Baker, R.; Grätzel, M. *J. Phys. Chem.* **1994**, *98*, 952.
- Hagfeldt, A.; Lindquist, S.-E.; Grätzel, M. *Sol. Energy Mater. Sol. Cells* **1994**, *32*, 245.
- Smestad, G. *Sol. Energy Mater. Sol. Cells* **1994**, *32*, 273.
- Rosenbluth, M.; Lewis, N. S. *J. Am. Chem. Soc.* **1986**, *108*, 4689.
- Yoon, K. J.; Min, H. J.; Kim, K. J. *J. Korean Chem. Soc.* **1992**, *36*, 107.
- Takeuchi, K. T.; Thompson, M. S.; Pipes, D. W.; Meyer, T. J. *Inorg. Chem.* **1984**, *23*, 1845.
- Kavarnos, G. J. *Fundamentals of Photoinduced Electron Transfer*; VCH Publ.; New York, 1993, p 312.
- Marcus, R. A. *J. Chem. Phys.* **1965**, *43*, 679.
- Pleskov, Y. V.; Gurevich, Y. Y. *Semiconductor Photo-electrochemistry*; Consultants Bureau; New York, 1986, p 220.
- Kumat, A. Ph.D. Thesis, Calif. Inst. Tech. 1992.
- MaO, D.; Kim, K. J.; Frank, A. J. *J. Electrochem. Soc.* **1994**, *141*, 1231.

facilitate the spreading of the colloid on the substrate. Using this solution, a 6 μm TiO_2 film was coated on ITO glass (Samsung Corning) by a spin-coating method at 3000 rpm and annealed at 500 $^\circ\text{C}$ in air for 1 hr.

Ga-In eutectic was rubbed on ITO in order to form ohmic contact with Cu wire. The contacts and the exposed edges of the electrode were insulated with an epoxy (K-epoxy, McKim Group). The area of the TiO_2 electrodes exposed to light was typically 1.0 cm^2 .

Synthesis of Ruthenium Complexes

[Ru(tpy)Cl₃](III)¹⁵. A 2.080 g amount of $\text{RuCl}_3 \cdot x\text{H}_2\text{O}$ and 0.240 g of 2,2':6'2"-terpyridine were heated at reflux for 4 hr in 250 mL absolute ethanol. Dark brown solid was collected from the red solution and washed with 30 mL of acetone, 50 mL of ether, and air-dried.

[Ru(tpy)(bpy(COOH)₂)Cl]Cl¹⁵. A 0.50 g quantity of Ru(tpy)Cl_3 and 0.30 g of 2,2'-bipyridine-4,4'-dicarboxylic acid were heated at reflux for 5 hr in 250 mL of 75% EtOH/25% H_2O containing 0.08 g of LiCl and 0.5 mL of triethylamine as a reductant. The pot contents were filtered hot and their volume was reduced to ~10 mL with a rotary evaporator, followed by chilling in a refrigerator for 24 hr. The solid was collected on a frit and washed with 50 mL ether and air-dried.

[Ru(tpy)(bqu(COOH)₂)Cl]Cl. The preparation was carried out by using the same procedure as for [Ru(tpy)(bpy(COOH)₂)Cl]Cl, substituting 2,2'-biquinoline-4,4'-dicarboxylic acid for the 2,2'-bipyridine-4,4'-dicarboxylic acid ligand.

[Ru(tpy)(bpy(COOH)₂)H₂O]Cl₂¹⁵. A 0.2 g amount of [Ru(tpy)(bpy(COOH)₂)Cl]Cl and 0.1 g of AgClO_4 were heated together at reflux for 1 hr in 100 mL of 75% acetone/25% H_2O . The solution volume was reduced to 10 mL with a rotary evaporator. The product was recrystallized in ethanol.

[Ru(tpy)(bpy(COOH)₂)CN]CN₅. A 0.3 g of [Ru(tpy)(bpy(COOH)₂)Cl]Cl and a 10-fold excess of KCN were heated at reflux and the solution volume was reduced with a rotary evaporator. The product was collected on a frit and recrystallized in ethanol.

Adsorption of ruthenium complexes to a TiO_2 electrode⁵. Each of ruthenium complex (0.010 g) was dissolved in 20 mL ethanol. Coating of the TiO_2 surface with a dye was carried out by soaking the TiO_2 film for 12 hr in the dye solution. It was resoaked in absolute ethanol to remove non-adsorbed dye molecules for 3 hr. The absorbance of adsorbed dye was determined by a UV-vis spectrophotometer.

Instruments and set-up

Photocurrents and cyclic voltammograms were obtained with an EG & G potentiostat/galvanostat M273. An Oriol 250W quartz tungsten halogen lamp (QTH) was served as a light source in conjunction with a Hitachi 390 nm cut-off filter to remove ultraviolet radiation. Light intensity was calibrated against a Newport 18/5-C power meter. The TiO_2 electrodes were illuminated in a three-electrode, one-compartment cell with a Pt mesh counter electrode and a Ag/AgCl reference electrode. The cell was made of pyrex fitted with 3 cm water jacket. In order to obtain monochromatic

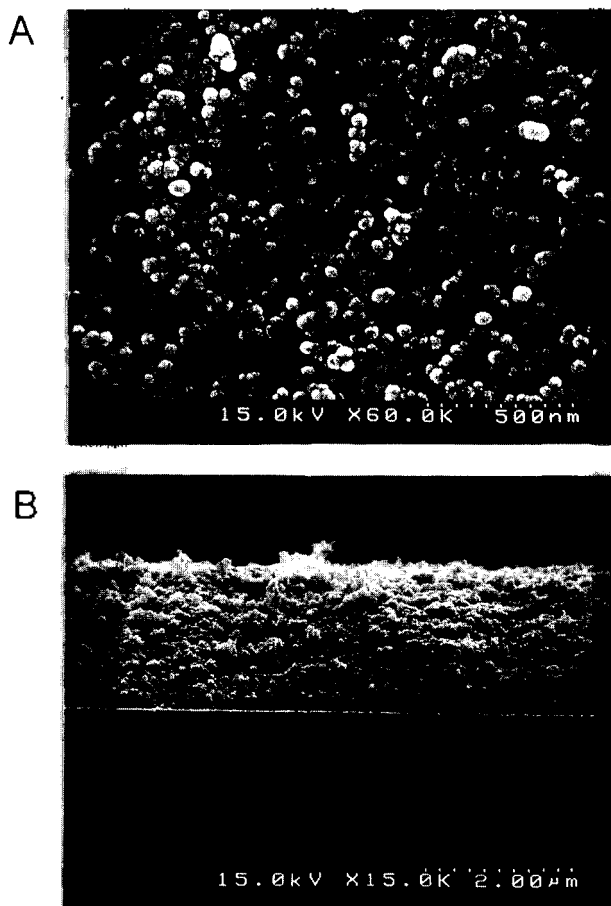


Figure 1. Scanning electron micrographs of a TiO_2 electrode deposited on a conducting glass. Magnification: (A) $\times 60,000$ (B) $\times 15,000$.

light a Bowman Series 2 luminescence spectrometer was used and UV-vis spectra were obtained with a Hewlett Packard 8452A diode array spectrophotometer. An ISI-SX-30E scanning electron microscope was employed to study the TiO_2 electrode surface and its thickness.

Results and Discussion

TiO_2 Film Characteristics

Figure 1 shows typical scanning electron micrographs of a TiO_2 film prepared by spin-coating colloidal TiO_2 particles on a conducting glass followed by annealing for 1 hr at 500 $^\circ\text{C}$. The sizes of TiO_2 particles in the film are quite uniform and estimated to be about 30–45 nm in diameter. The thickness of the TiO_2 films increases with the number of spin coating. The average thickness per spin coating was measured to be about 0.6 μm . With an increase in the film thickness the absorption spectra of the TiO_2 films show a red shift (Figure 2a). The absorbances at longer wavelengths are due to the decrease in transmittance caused by a somewhat hazy nature of the film. The absorbance of the dye-coated TiO_2 film corrected for the TiO_2 absorption and divided by the molar absorptivity yielded the surface dye concentration of about 2.3×10^{-7} mol/ cm^2 for a 6 μm -thick TiO_2 film. The photoelectrochemical behavior of spin-coat-

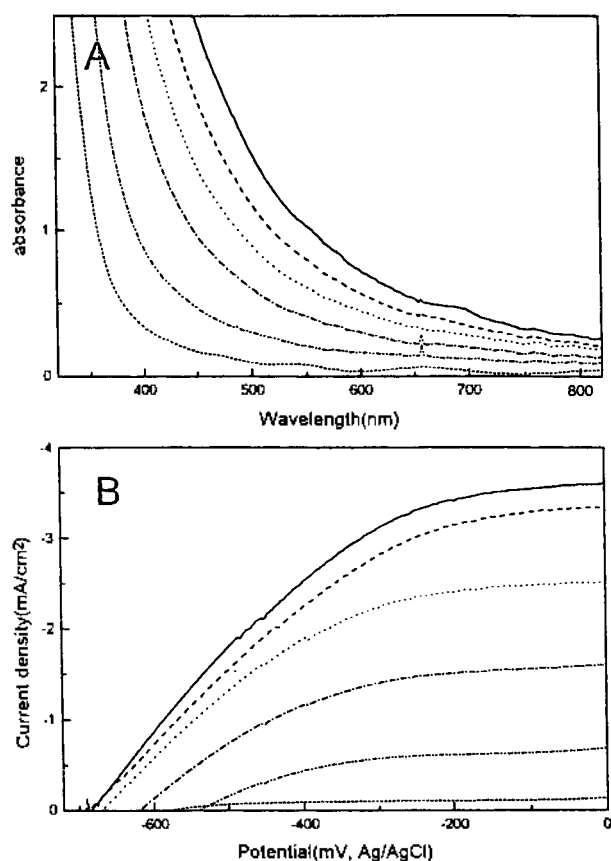


Figure 2. UV-vis spectra of bare TiO₂ electrodes and (B) current density-potential curves of Ru(tpy)(bpy(COOH)₂CN)⁺/TiO₂ anodes vs. film thickness in 0.3 M LiI/0.03 M I₂ acetonitrile solution at 100 mW/cm². — (9.0 μm), --- (7.2 μm), (5.4 μm), - - - (3.6 μm), - · - · (1.8 μm), ····· (0.6 μm).

ed TiO₂ films was studied by monitoring the photocurrent generated in a cell that employed a TiO₂ photoanode, a Pt mesh counter electrode, and I⁻/I₃⁻ as the redox electrolyte in acetonitrile. Figure 2b displays the current densities vs. applied potential of the TiO₂ film with different thickness using a ruthenium complex Ru(tpy)(bpy(COOH)₂CN)⁺ as a sensitizer. Higher current densities were obtained with the increase in the film thickness due to the increased adsorption of the ruthenium complex on the TiO₂ particles having high porosity and surface-to-volume ratio. A roughness factor, defined as the ratio between the real and projected surface of the film, of about 1000 has been obtained.² It appears to be desirable to have a thick film of TiO₂ in a photoelectrochemical cell in order to have a high photocurrent. However, as the thickness increases the injected electrons from the excited ruthenium complexes into the conduction band of TiO₂ become more difficult to migrate to the ITO substrate, and become easier to recombine with the oxidized ruthenium complexes or with oxidized species in the electrolyte solution. Similar explanation may be applied to the open-circuit photovoltage, V_{oc} , which is the voltage obtained at zero current density. The results in Figure 2b illustrates that V_{oc} reaches a steady value, about 0.68 V, beyond which the enhanced recombination appears to compensate with the increase in the injected electrons.

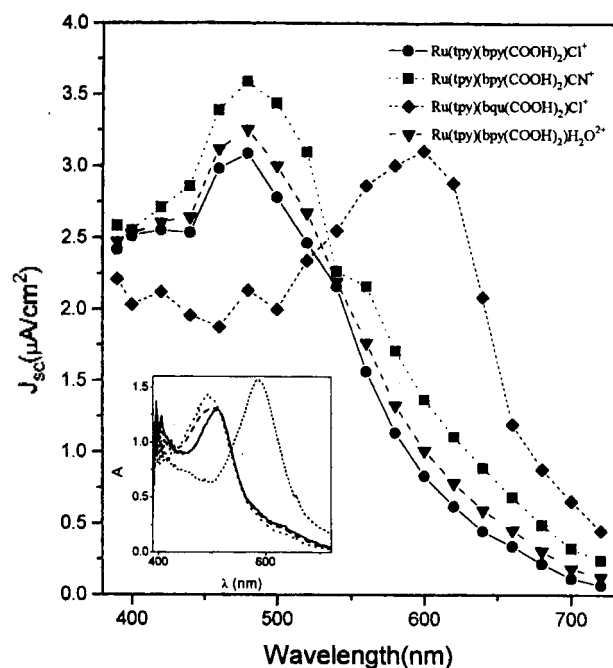


Figure 3. Photocurrent action spectra of Ru complex-sensitized TiO₂ electrode in 0.3 M LiI/0.03 M I₂ acetonitrile solution. The inset shows the absorption spectra of Ru complexes adsorbed on TiO₂ electrodes.

The current action spectra obtained with the TiO₂ films coated with the four ruthenium complexes are shown in Figure 3. Also shown are the absorption spectra of the dye-coated TiO₂ films. The photocurrent action spectra resemble their absorption spectra, indicating that under visible light illumination the ruthenium sensitizers are excited and the photogenerated electrons are transported efficiently to ITO through the nanocrystalline TiO₂ film.

Dye-Sensitization

Figure 4 shows the current density-voltage characteristics obtained with a photoelectrochemical cell that employed 6 μm thick, spin coated TiO₂ in 0.3 M LiI/0.030 M I₂ acetonitrile under visible-light illumination at 45 mW/cm² as described in Experimental. The TiO₂ electrodes were coated with the ruthenium sensitizers prior to the measurement of the photoelectrochemical behavior. The results of Figure 4 are tabulated in Table 1 with respect to the open-circuit voltage V_{oc} , short-circuit current density J_{sc} , fill factor ff , and conversion efficiency η . Table 1 also includes the half-wave potentials $E_{1/2}$ of the ruthenium complexes which were obtained by cyclic voltammetry in 1.0 M LiClO₄ acetonitrile.

The data in Table 1 show that among the sensitizers studied Ru(tpy)(bpy(COOH)₂CN)⁺ yielded the largest V_{oc} , J_{sc} , and η whereas Ru(tpy)(bqu(COOH)₂Cl produced the least conversion efficiency.

The variations in J_{sc} for the sensitizers can be attributed to the difference in the rate of heterogeneous charge transfer from the excited sensitizer, the donor, to the conduction band of TiO₂ the acceptor. For the electron transfer, there exists a free energy of activation for which the rate of the electron transfer is maximal. Under the present experimental conditions, we may assume that the Coulombic interactions

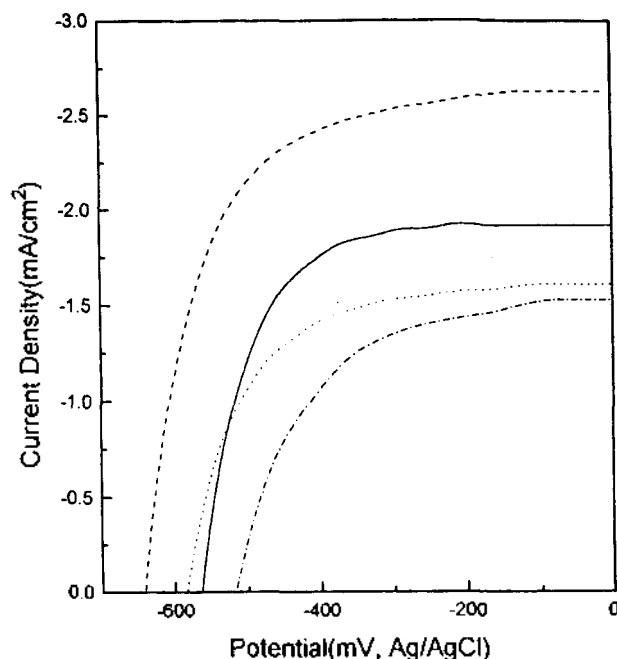


Figure 4. Photocurrent density-potential curves of Ru complexes adsorbed on the TiO_2 electrodes in 0.3 M LiI/0.03 M I_2 acetonitrile solution at 45 mW/cm^2 light intensity. — $\text{Ru}(\text{tpy})(\text{bpy}(\text{COOH})_2)\text{H}_2\text{O}^{2+}$, ---- $\text{Ru}(\text{tpy})(\text{bpy}(\text{COOH})_2)\text{CN}^+$, $\text{Ru}(\text{tpy})(\text{bpy}(\text{COOH})_2)\text{Cl}^+$, - · - · $\text{Ru}(\text{tpy})(\text{bqu}(\text{COOH})_2)\text{Cl}^+$.

between the cationic ruthenium complexes and the TiO_2 electrode are essentially the same and the ruthenium complexes are anchored to the TiO_2 surface by the carboxylate groups in the bipyridyl ligands. In addition, we may neglect the differences in the regeneration of the oxidized dyes by the electron transfer from iodide ions, because of relative slowness of the back reaction,² and because of nearly identical ionic atmospheres around ruthenium in the sensitizers of similar size with respect to the access of iodide ions. Figure 5 represents the energy level of the conduction band edge and the Fermi level of TiO_2 . Also shown are the ground and the excited state levels of the sensitizers which were established by cyclic voltammetry and absorption spectroscopy, respectively (Table 1). The energy difference between the two levels of the sensitizer approximately corresponds to the absorption maximum wavelength. The sensitizer $\text{Ru}(\text{tpy})(\text{bpy}(\text{COOH})_2)\text{CN}^+$ has the largest energy difference possibly because CN^- is a stronger ligand than Cl^- or H_2O in the spectrochemical series. It is immediately evi-

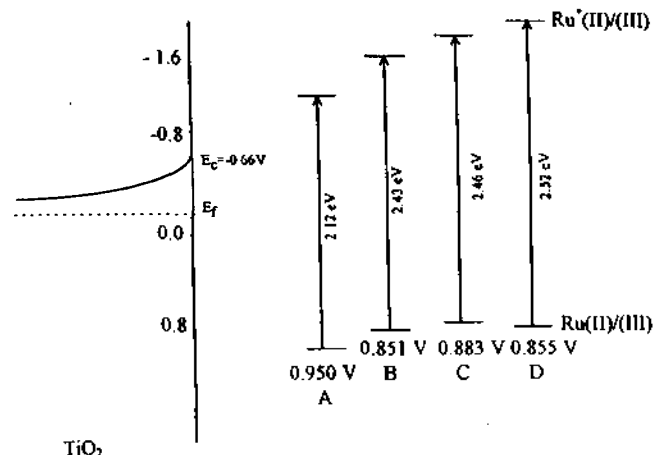


Figure 5. Interface energetics for TiO_2 thin films and Ru complexes in acetonitrile. A: $\text{Ru}(\text{tpy})(\text{bqu}(\text{COOH})_2)\text{Cl}^+$, B: $\text{Ru}(\text{tpy})(\text{bpy}(\text{COOH})_2)\text{Cl}^+$, C: $\text{Ru}(\text{tpy})(\text{bpy}(\text{COOH})_2)\text{H}_2\text{O}^{2+}$, D: $\text{Ru}(\text{tpy})(\text{bpy}(\text{COOH})_2)\text{CN}^+$.

dent on inspecting Table 1 and Figure 5 that the highest current density was obtained with the sensitizer whose excited state energy lies farthest from the conduction band edge of TiO_2 , whereas the lowest current density was obtained with the sensitizer lying closest to the conduction band edge. The increasing order of the current density of ruthenium dyes agrees well with the increase in the energy difference of the dyes. Therefore the energy difference between the conduction band edge and the excited state of the sensitizer can be regarded as a measure of the rate of the heterogeneous electron transfer.

The current density data can be interpreted by employing the free energy of activation, ΔG^\ddagger_{et} , a potential barrier associated with the heterogeneous electron transfer from the excited sensitizer to TiO_2 . The existence of a potential barrier is not unreasonable since the electron transfer should involve the injection of electrons from the bipyridyl ligand through the carboxylate group into the conduction band of TiO_2 .

For the case of photoinduced electron transfer on a semiconductor the rate of electron transfer can be described as,¹⁶

$$k \propto \exp(-\Delta G^\ddagger_{et}/RT) \quad (1)$$

where ΔG^\ddagger_{et} is the free energy of activation for the electron transfer and is related to the driving force, ΔG_{et} , which is the energy difference between the excited state and the conduction band of TiO_2 ,¹⁷

$$\Delta G^\ddagger_{et} = \frac{\lambda}{4} \left(1 + \frac{\Delta G_{et}}{\lambda} \right)^2 \quad (2)$$

where λ is defined as the total reorganization energy. This parameter can be separated into two terms, $\lambda = \lambda_v + \lambda_s$, where λ_v refers to the energy changes accompanying changes in bond lengths and bond angles during the electron-transfer step and λ_s refer to the energy change as the solvent shells surrounding the reactants rearrange. However, the variations of λ_s in identical solution are apparently insignificant since the radii of the sensitizers are very much the same. Thus

Table 1. V_{oc} , J_{sc} , ff , and $E_{1/2}$ (mV vs Ag/AgCl) of TiO_2 electrodes sensitized by ruthenium complexes. Incident light intensity was 45 mW/cm^2

| Complex | V_{oc} (V) | J_{sc} (mA/cm^2) | ff | $E_{1/2}^a$ | η (%) |
|---|-----------------|---|------|-------------|------------|
| $\text{Ru}(\text{tpy})(\text{bpy}(\text{COOH})_2)\text{Cl}^+$ | 0.59 | 1.8 | 0.54 | 851 | 1.3 |
| $\text{Ru}(\text{tpy})(\text{bpy}(\text{COOH})_2)\text{CN}^+$ | 0.64 | 2.7 | 0.52 | 855 | 2.0 |
| $\text{Ru}(\text{tpy})(\text{bpy}(\text{COOH})_2)\text{H}_2\text{O}^{2+}$ | 0.57 | 2.1 | 0.54 | 833 | 1.4 |
| $\text{Ru}(\text{tpy})(\text{bqu}(\text{COOH})_2)\text{Cl}^+$ | 0.52 | 1.5 | 0.51 | 950 | 0.9 |

^a in mV measured from 0.1 M LiClO₄, acetonitrile.

ΔG^\ddagger should be a function of the differences in equilibrium bond distances between the sensitizer and its oxidized species, and the force constants for all the vibrations of a reactant and product molecule.¹⁶ Apparently, in the present system, λ in a collective manner is somehow manifested to make ΔG^\ddagger_{et} smaller as ΔG_{et} becomes larger for the ruthenium complexes. Then it is expected that the higher the energy of the excited state, the smaller the effective potential barrier, and the larger is the current density. The back reaction is known to be much smaller compared with the electron-transfer reaction.² The applied potential provides a driving force for electron collection and prevents the charge recombination. Depending on the direct coordination of the sensitizer molecules onto the surface of TiO₂, the excited state of the sensitizer can be stabilized in comparison with the level predicted from the absorption spectrum. Then the potential barrier can be significantly lowered.

The maximal attainable photovoltage is the difference between the quasi Fermi level of TiO₂, F_n , and the electrochemical potential of the electrolyte I^-/I_3^- , E_{redox} .² Variation in the measured V_{oc} (Table 1) therefore resulted from the difference in the quasi Fermi level, which was caused by the non-equilibrium stationary concentration of the conduction band electrons during illumination, n^* . The rise of F_n with respect to E_{redox} is possibly expressed by¹⁸

$$F_n - E_{redox} \approx kT \ln \frac{\Delta n}{n_0} \quad (3)$$

where $\Delta n = n^* - n_0$ and n_0 is the concentration of the conduction band electrons under equilibrium in the dark. Since Ru(tpy)(bpy(COOH)₂)CN* produced the highest current density, its Δn is expected to be largest under the open circuit. As a consequence, V_{oc} of Ru(tpy)(bpy(COOH)₂)CN* should be the largest. Similarly, the smallest V_{oc} of Ru(tpy)(bpy(COOH)₂)Cl* can be related to its lowest current density among the sensitizers studied.

The plots in Figure 6 were based on the experimental data obtained for the dependence of current density-potential curves on the incident light intensities. From the plots a linear relationship between V_{oc} and $\log(J_{sc})$ holds up to about 7 mA/cm² for Ru(tpy)(bpy(COOH)₂)CN* and about 3 mA/cm² for other ruthenium complexes. The observation of the linear relationship suggests that the present photoelectrochemical cells under sub-bandgap illumination behave similarly to a diode under forward bias. Under open circuit, the photogenerated current is balanced by the recombination current. The open circuit photovoltage (V_{oc}) is related with J_{sc} by^{5,19,20}

$$V_{oc} = \frac{AKT}{q} \ln \frac{J_{sc}}{J_0} \quad (4)$$

where A is a parameter known as the diode quality factor, and J_0 is the saturation current density.²⁰ The value of A is dependent upon the transport mechanism that controls J_0 . With the aid of Eq. 4, the diode quality factors are obtained from the linear range of the plots in Figure 6, and found to be 2.3 ± 0.1 for all the ruthenium complexes. The number of investigations that report the diode quality factor for regenerative photoelectrochemical cells is limited.^{5,12,20} Recently, in similar studies to ours using *cis*-di(thiocyanato)bis(2,2'-bipyridyl-4,4'-dicarboxylate)ruthenium(II) as a sensitiz-

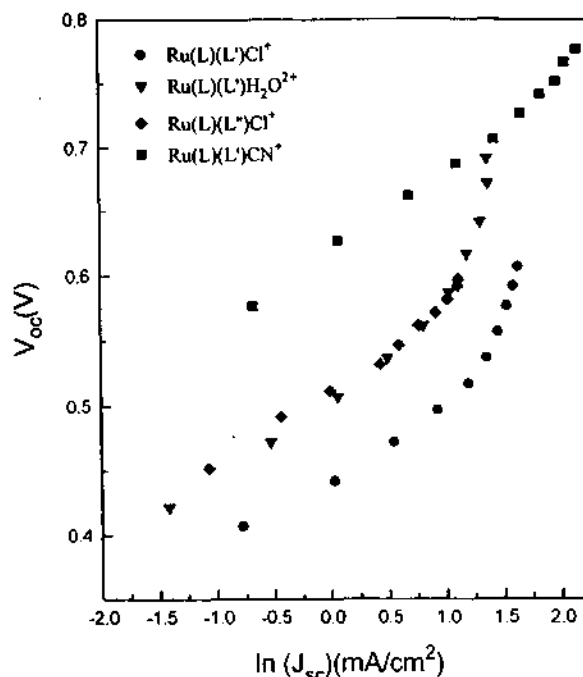
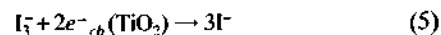


Figure 6. Plot of open-circuit potentials of dye/TiO₂ electrodes against short-circuit currents. L=terpyridine, L'=2,2'-bipyridine-4,4'-dicarboxylic acid, L''=2,2'-biquinoline-4,4'-dicarboxylic acid.

er, Nazeeruddin *et al.* described the performance characteristics of a TiO₂ cell where the diode quality factor was not given explicitly, but deduced to be about 1.4.⁵ Their explanation was mainly concerned with the recombination current caused by the reduction of triiodide ions in the electrolyte by the conduction band electrons,



Triiodide ion can penetrate into the nanometer-sized pores due to its relatively small size. However, if this recombination mechanism dominates, the diode quality factor should be 1.0¹³ instead of 1.4. The discrepancy arises because the current does not flow predominantly by the triiodide reduction. This discrepancy and the even larger A obtained in this study imply that other recombination mechanisms should participate in the present system. With a slightly different type of ruthenium dye, Smestad measured A=1.6.¹² This rather high value of A was attributed to both the triiodide reduction (Eq. 5) and the back reaction of the electron injection via recombination centers and surface states. Perhaps the surface recombination by trapping centers would be worthwhile to investigate extensively.¹⁹

Figure 7 shows the conversion efficiencies as a function of incident light intensity. Because we did not take into account the loss of light intensity due to the reflection off the glass surface of the photoelectrochemical cell and light absorption by the redox electrolyte, the relative conversion efficiencies of the TiO₂ electrodes were considered to be more relevant in this study. For all light intensities, Ru(tpy)(bpy(COOH)₂)CN* showed the highest conversion efficiencies, whereas Ru(tpy)(bpy(COOH)₂)Cl* had the lowest conversion efficiencies, except for the low light intensity region, which is consistent with the data present above. At

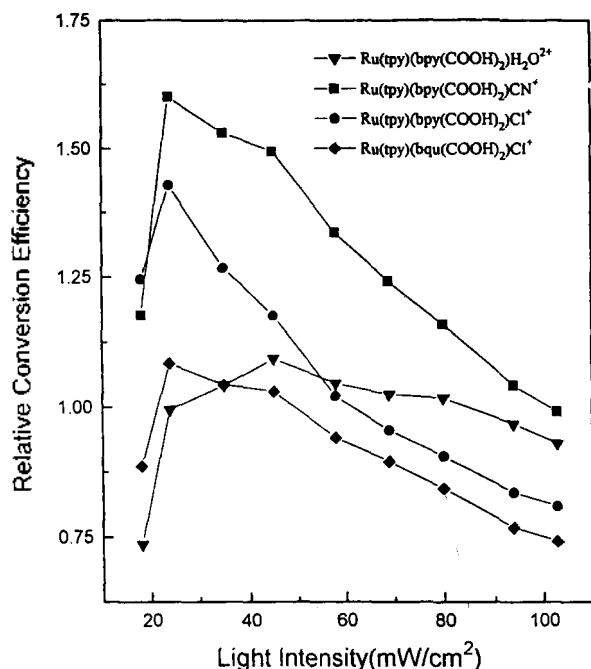


Figure 7. Dependence of light-to-current conversion efficiencies on incident light intensity.

higher intensities (above approximately 45 mW/cm²) under the present conditions the conversion efficiencies fall off rapidly, suggesting that the recombination of the injected electrons prevails over the diffusion by the conduction band electrons toward the TiO₂/ITO interface.

Stability of the Photocurrent

In order to examine the stability of the photoelectrochemical cell, the time dependence of the current density was measured. With the sensitizer Ru(tpy)(bqu(COOH)₂)Cl⁻ we observed that the current density decreased by about 86% during the first 60 min period, while the other three sensitizers possessing bipyridyl ligands showed about a 55% decrease under the same conditions. The poor stabilities can mainly be attributed to the accumulation of oxidized dyes on the TiO₂ surface and the slow regeneration of reduced dyes by the electron transfer from I₃⁻. Since Ru(tpy)(bqu(COOH)₂)Cl⁻ is expected to have a more hydrophobic atmosphere than the other dyes, the accumulation will be largest. Another possibility for the fast decay of the current density may arise from the complexation of I₃⁻ with the oxidized Ru(II) complexes, which hinders the electron transfer. Upon prolonged illumination, the degradation of Ru(II) complexes may also contribute to the poor stabilities. Further studies are needed to clarify the causes.

Conclusion

Dye-sensitized photocurrent densities were measured from nano-crystalline TiO₂ in acetonitrile. Ru(tpy)(bpy(COOH)₂)CN⁻ showed higher photocurrent density than other ruthenium complexes of similar structure. The results were interpreted by employing a potential barrier between the charge transfer excited state of a dye and the conduction band of TiO₂. The potential barrier should be a complex

function of the energy change accompanying predominantly the changes in chemical bond lengths during the electron transfer step. The energy change as the solvents around the reactants rearrange is insignificant. Ru(tpy)(bpy(COOH)₂)CN⁻ also produced a higher open-circuit photovoltage than the other sensitizers, implying that the quasi Fermi level lies the highest. A high diode quality factor suggests that a surface recombination process by trapping centers and surface states should be included in the recombination mechanism in addition to the reduction of triiodide by the injected conduction band electrons.

Acknowledgment. This work was supported by the Korea Science and Engineering Foundation (94-0501-05-01-3) and partially by the Ministry of Trade, Industry and Energy.

References

- Grätzel, M.; Kalyanasundaram, K. In *Photosensitization and Photo-catalysis Using Inorganic and Organometallic Compounds*; Klumer Academic Publ.: Dordrecht, The Netherlands, 1993; p 247.
- Hagfeldt, A.; Grätzel, M. *Chem. Rev.* **1995**, *95*, 49.
- Tan, M. S.; Laibinis, P. E.; Nguyen, S. T.; Kesselman, J. M.; Stanton, C. E.; Lewis, N. S. In *Progress in Inorganic Chemistry*; Karlin, K. D., Ed.; John Wiley: New York, USA, 1994; Vol. 41, p 21.
- O'Regan, B.; Grätzel, M. *Nature(London)*, **1991**, *353*, 737.
- Nazeeruddin, M. K.; Kay, A.; Humphry-Baker, R.; Müller, E.; Liska, P.; Vlachopoulos, N.; Grätzel, M. *J. Am. Chem. Soc.* **1993**, *115*, 6382.
- Bonhôte, P.; Moser, J. E.; Vlachopoulos, N.; Walder, L.; Zakeeruddin, S. M.; Humphry-Baker, R.; Grätzel, M. *Chem. Commun* **1996**, 1163.
- Péchy, P.; Rotzinger, F. P.; Nazeeruddin, M. K.; Kohle, O.; Zakeeruddin, S. M.; Humphry-Baker, R.; Grätzel, M. *J. Chem. Soc. Chem. Commun* **1995**, 65.
- Vogel, R.; Hoyer, P.; Weller, H. J. *J. Phys. Chem.* **1994**, *98*, 3183.
- Spitler, M. T.; Calvin, M. *J. Chem. Phys.* **1977**, *66*, 1294.
- Kay, A.; Humphry-Baker, R.; Grätzel, M. *J. Phys. Chem.* **1994**, *98*, 952.
- Hagfeldt, A.; Lindquist, S.-E.; Grätzel, M. *Sol. Energy Mater. Sol. Cells* **1994**, *32*, 245.
- Smestad, G. *Sol. Energy Mater. Sol. Cells* **1994**, *32*, 273.
- Rosenbluth, M.; Lewis, N. S. *J. Am. Chem. Soc.* **1986**, *108*, 4689.
- Yoon, K. J.; Min, H. J.; Kim, K. J. *J. Korean Chem. Soc.* **1992**, *36*, 107.
- Takeuchi, K. T.; Thompson, M. S.; Pipes, D. W.; Meyer, T. J. *Inorg. Chem.* **1984**, *23*, 1845.
- Kavarnos, G. J. *Fundamentals of Photoinduced Electron Transfer*; VCH Publ.; New York, 1993, p 312.
- Marcus, R. A. *J. Chem. Phys.* **1965**, *43*, 679.
- Pleskov, Y. V.; Gurevich, Y. Y. *Semiconductor Photo-electrochemistry*; Consultants Bureau; New York, 1986, p 220.
- Kumat, A. Ph.D. Thesis, Calif. Inst. Tech. 1992.
- MaO, D.; Kim, K. J.; Frank, A. J. *J. Electrochem. Soc.* **1994**, *141*, 1231.